# A Second-Order Cone Programming (SOCP) Based Optimal Power Flow (OPF) Model with Cyclic Constraints for Power Transmission Systems

Md Mahmud-Ul-Tarik Chowdhury, *Student Member, IEEE,* Sukumar Kamalasadan, *Senior Member, IEEE,* and Sumit Paudyal, *Senior Member, IEEE*

***Abstract*—For meshed power networks, even though the conic relaxation is shown to be exact, the relaxation of angles may not be exact using the existing Second-Order Cone Programming (SOCP) based optimal power flow (OPF) models. Power transmission networks generally have mesh orientation, and the cyclic angle constraints are not satisfied with the existing SOCP-OPF models. This work proposes a SOCP-OPF model for power transmission networks that satisfies the cyclic angle constraints for any mesh in the network. The novelty of the proposed OPF model is that it defines a convex envelope to represent the relative bus voltage angles that satisfy the cyclic constraint criteria for a mesh network. The proposed SOCP-OPF model is tested on the IEEE 14-bus, 57-bus, 118-bus, 500-bus, and 2736-bus networks. The case studies demonstrate that the proposed model is computationally efficient and scalable for large transmission networks compared to the Nonlinear Programming (NLP) and semi-definite programming (SDP) counterparts.**

***Index Terms*—Optimal power flow (OPF), convex relaxation, second-order conic programming (SOCP), cyclic constraints, and transmission networks.**

## NOMENCLATURE

| | |
|---|---|
| $\mathcal{L}$ | Set of all the branches in the network |
| $\mathcal{N}$ | Set of all the buses in the network |
| $\mathcal{N}_g$ | Set of all the buses with generators in the network |
| $\overline{()}$ | maximum limits of the variables and parameters |
| $\theta_{ij}$ | Bus voltage angle difference between the bus $i \in \mathcal{N}$ and bus $j \in \mathcal{N}$ |
| $\underline{()}$ | minimum limits of the the variables and parameters |
| $\overline{B}_{ij}$ | Imaginary part of the off-diagonal components of the network admittance matrix ($Y$) |
| $c_2^i, c_1^i$ & $c_0^i$ | Cost coefficients for the generator at bus $i \in \mathcal{N}_g$ |
| $G_{ij}$ | Real part of the off-diagonal components of the network admittance matrix ($Y$) |
| $I_{ij}$ | Current flow through a branch $L_{ij} \in \mathcal{L}$ connecting the bus $i \in \mathcal{N}$ and bus $j \in \mathcal{N}$ |
| $l_{ij}$ | Magnitude square of the current flow through a branch $L_{ij} \in \mathcal{L}$ connecting the bus $i \in \mathcal{N}$ and bus $j \in \mathcal{N}$ |
| $P_i^d$ | Real power demand at the bus $i \in \mathcal{N}$ |
| $P_i^g$ | Real power injection at the bus $i \in \mathcal{N}_g$ |
| $P_{ij}$ | Real power flow through the branch $L_{ij} \in \mathcal{L}$ connecting the bus $i \in \mathcal{N}$ and bus $j \in \mathcal{N}$ |
| $Q_i^d$ | Reactive power demand at the bus $i \in \mathcal{N}$ |
| $Q_{ij}$ | Reactive power flow through the branch $L_{ij} \in \mathcal{L}$ connecting the bus $i \in \mathcal{N}$ and bus $j \in \mathcal{N}$ |
| $Q_i^g$ | Reactive power injection at the bus $i \in \mathcal{N}_g$ |
| $S_i^g$ | Apparent power at the bus $i \in \mathcal{N}_g$ |
| $S_i^d$ | Apparent power demand at the bus $i \in \mathcal{N}$ |
| $S_{ij}$ | Apparent power flow through the branch $L_{ij} \in \mathcal{L}$ connecting the bus $i \in \mathcal{N}$ and bus $j \in \mathcal{N}$ |
| $u_i$ | Magnitude square of the voltage at the bus $i \in \mathcal{N}$ |
| $V_i$ | Voltage at the bus $i \in \mathcal{N}$ |
| $z_{ij}$ | Impedance of the branch $L_{ij} \in \mathcal{L}$ connecting the bus $i \in \mathcal{N}$ and bus $j \in \mathcal{N}$ |

This work is supported in part by the NSF grants ECCS-1810174 and ECCS-2001732. M. M. Chowdhury and S. Kamalasadan are with the Department of Electrical Engineering, The University of North Carolina at Charlotte, USA. S. Paudyal is with the Department of Electrical Engineering, Florida International University, Miami, USA. Emails: mchowdh6@uncc.edu, skamalas@uncc.edu, spaudyal@fiu.edu. Corresponding Author: Md Mahmud-Ul-Tarik Chowdhury (Email: mchowdh6@uncc.edu).

## I. INTRODUCTION

OPTIMAL Power Flow (OPF) analysis is one of the salient tools in power system planning and operation for particular objectives (e.g., generation costs, power losses) by maintaining the bus voltages and branch flows within the operational limits [1]–[3]. OPF analysis is typically formulated using AC power flow equations considering multiple operational constraints, referred to as AC-OPF. Due to the non-convexity of power flow equations and network constraints, the AC-OPF problem originally is non-deterministic polynomial (NP)-hard [4], [5]. Moreover, the non-convexity in AC-OPF formulation leads to computational intractability, particularly for large power networks; thus, a globally optimal solution may not be guaranteed [3], [6]. Conventionally, linear approximations of power flow equations are commonly used to overcome the computational challenges of the non-convex AC-OPF formulations. However, approximation of linear formulations like DC-OPF [7], [8] compromise the solution accuracy. Thus, the solutions from such formulations may not be optimal.

On the contrary, the convex relaxations of AC-OPF problems are conditionally exact (hence, AC-feasible) and computationally efficient [9]. Due to the ability to find global optima, the convex AC-OPF formulations have been extensively used in various power system optimization applications [10]–[12]. Additionally, the convex envelopes have been a promising approach for the non-linear terms in OPF analysis [13]. However, it was noted that the accuracy of the convex relaxations depends on the tightness of these convex envelopes [14]. A robust convex restriction to solve robust OPF problems is introduced in [15]. To this end, sufficient conditions for the exactness of the relaxations are illustrated in [16], [17]. Among the variants of convex OPF formulations, the second-order cone programming (SOCP) [18], and semi-definite programming (SDP) [19] based models are used commonly for

OPF problems. SOCP-based load flow formulation was first proposed for radial distribution networks in [18], and a conic quadratic model was proposed in [20] for meshed networks. For the SOCP-OPF model, the angle and conic relaxations are exact in radial networks with no upper bounds on loads.

In the mesh networks, angle relaxation of AC-OPF can be inexact as the cyclic constraints are not satisfied (i.e., the sum of voltage angle difference around any loop should be zero) [21]. The conditions for the angle recovery for the SOCP-OPF model are discussed in [22], [23]. Three methods are proposed in [21] for enhancing the original SOCP-OPF model for mesh networks that ensure the cyclic constraints for the mesh networks. However, the model suffers computational challenges for large meshed networks. In [24], instead of considering the cyclic constraints directly for the meshed networks, an alternative SOCP-OPF model using difference-of-convex programming (DCP) is used, which requires convex-concave procedure (CCP) based iterations. A SOCP-OPF model is proposed with relaxation by generating new cutting planes using SDP relaxation in [25]. Though the SDP cuts effectively exclude infeasible solutions and enhance the SOCP relaxation of OPF, they add computational burden on the solution process. Reference [26] proposes relaxation of the cyclic constraints, where a higher-order moment relaxation matrix for each maximal clique is formed to satisfy the cyclic constraints. In conclusion, the existing SOCP-OPF models face challenges with the cyclic constraints for tight and scalable OPF methods for the meshed networks.

On the other hand, SDP formulation retains the angle information and can find an exact solution of OPF analysis for meshed networks with certain conditions and limitations [27], [28]. So, SDP relaxations are theoretically more robust [25] compared to SOCP relaxations for meshed transmission networks. However, the matrix size grows as the square of the number of buses in SDP leads to a high computational need for large networks [29]. In addition, SDP formulations find a physically meaningful OPF solution if the line-flow limits are not binding [30]. However, SOCP relaxation-based OPF models are shown to be computationally efficient for large networks [13].

From the above discussion, the SOCP is computationally efficient but suffers from angle relaxation for meshed power networks due to the cyclic angle constraints. This motivates our proposed work to consider cyclic constraints directly in the SOCP AC-OPF formulation to obtain exact OPF solutions for mesh networks. With this premise, this paper proposes a convex envelope to retrieve and include the bus voltage angle difference across the branches that satisfies the cyclic constraints in any mesh cycle in the power network. Additionally, the branches that do not belong to any mesh follow the radial network approach as [31], [32] to determine the bus voltage phase difference for a tighter envelope. The bus voltage phase angle difference is recovered after the optimization if a wide envelope is considered. In the proposed approach, the voltage and current phase angles are first relaxed for converting the non-convex power flow equations into convex form. Then, a quadratic equation is relaxed as a second-order conic inequality constraint. Finally, a convex envelope has been derived for the bus voltage angle difference, adhering to the cyclic constraints of any mesh cycle in the network. The main contributions of the proposed model are as follows:

- A convex envelope is proposed to retrieve the bus voltage angle difference for all the branches in a power network. The envelope is determined based on the optimal power flow and the voltage limits. With the proposed OPF model, the bus voltage angle difference remains within the envelope and satisfies the mesh cyclic constraints.
- A theoretical framework, including the mathematical proof is developed for the relaxation of meshed power networks with the angle cyclic constraints.
- The approach also proposes a graph theory-based model for extracting the mesh cycles from a power network. The mesh cycles are determined from a network ex-ante of the SOCP-OPF analysis.

The paper is organized as follows. Section II discusses the proposed methodology, including the mathematical modeling in the relaxation framework and the graph theory-based cycle extraction method. The impacts of line flow limits on the SDP and SOCP-OPF models are illustrated in Section III. Section IV analyzes the exactness and global optimality of the proposed model. Section V discusses the model implementation and result evaluation, and Section VI concludes the paper.

## II. Proposed Methodology

It is well known that power transmission networks are generally in mesh orientation. Thus for generic model development, a small section of a meshed transmission network is considered as represented in the schematic diagram in Fig. 1. In this article, '$\mathcal{L}$' is considered as the set of all branches, and $\mathcal{N}$ is the set of all buses of the network. Further, $i$ and $j \in \mathcal{N}$ denote the bus index, and $L_{ij} \in \mathcal{L}$ denotes the branch connecting the bus $i \in \mathcal{N}$ and bus $j \in \mathcal{N}$.

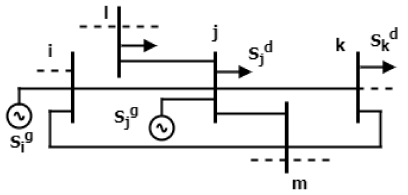


Fig. 1. Schematic diagram of a simple mesh network.

### A. Branch Flow Model (BFM) in Power System

Considering the above notations, the power flow relation through a branch $L_{ij} \in \mathcal{L}$ and voltage relations between the bus $i \in \mathcal{N}$ and bus $j \in \mathcal{N}$ can be represented as follows:

$$S_{ij} = V_i I_{ij}^* \tag{1}$$

$$V_j = V_i - \frac{z_{ij} S_{ij}^*}{V_i^*} \tag{2}$$

where $z_{ij}$ is the impedance of the branch $L_{ij} \in \mathcal{L}$. $S_{ij}$ and $I_{ij}$ represent the apparent power and current flow from bus $i \in \mathcal{N}$ to bus $j \in \mathcal{N}$ through the branch $L_{ij} \in \mathcal{L}$, respectively. The power balance equation at the bus $j \in \mathcal{N}$ is as follows:

$$S_j^g - S_j^d = \sum_{k:j \rightarrow k} S_{jk} - \sum_{i:i \rightarrow j} (S_{ij} - z_{ij}|I_{ij}|^2) + y_j^*|V_j|^2 \tag{3}$$

where $y_j = g_j + jb_j$ is the half lump shunt admittance equivalent of the line at the bus $j \in \mathcal{N}$. Let $Y$ denotes the admittance matrix of a power network, which has off-diagonal components as $Y_{ij} = G_{ij} + jB_{ij}$ for each branch $L_{ij} \in \mathcal{L}$ of the network. The real and reactive power flow through a branch $L_{ij} \in \mathcal{L}$ between two buses $i \in \mathcal{N}$ and $j \in \mathcal{N}$ can be represented as:

$$P_{ij} = -G_{ij}V_i^2 + G_{ij}V_iV_j\cos(\theta_{ij}) + B_{ij}V_iV_j\sin(\theta_{ij}) \quad (4)$$

$$Q_{ij} = B_{ij}V_i^2 - B_{ij}V_iV_j\cos(\theta_{ij}) + G_{ij}V_iV_j\sin(\theta_{ij}) \quad (5)$$

where $\theta_{ij} = \theta_i - \theta_j$; $\theta_i$ and $\theta_j$ are the bus voltage phase angle at the bus $i$ and $j \in \mathcal{N}$ respectively. Further, from (4) and (5):

$$V_iV_j\sin\theta_{ij} = \frac{B_{ij}P_{ij} + G_{ij}Q_{ij}}{G_{ij}^2 + B_{ij}^2} \quad (6)$$

Eqn. (6) shows the dependency of the bus voltage angle difference on the power flow through a branch in the network.

### B. Relaxation and Inclusion of Cyclic Constraints

*1) Angle Relaxation:* In the proposed convex model, to convexify (1)-(3), the phase angle of the voltage and the current are relaxed as, $I_{ij} \Rightarrow |I_{ij}|$ and $V_i \Rightarrow |V_i|$. New variables have been introduced as $|I_{ij}|^2 = l_{ij}$; $|V_i|^2 = u_i$ and $|V_j|^2 = u_j$. The equation in (1) is converted as follows:

$$u_il_{ij} = S_{ij}^2 \quad (7)$$

Considering the magnitude squared in (2), the voltage relationship between the bus $i \in \mathcal{N}$ & bus $j \in \mathcal{N}$ is as follows:

$$|V_j|^2 = |V_i|^2 + |z_{ij}|^2|I_{ij}|^2 - (z_{ij}S_{ij}^* + z_{ij}^*S_{ij}) \quad (8)$$

With the new variable as $|I_{ij}|^2 = l_{ij}$; $|V_i|^2 = u_i$ and $|V_j|^2 = u_j$ for the squared terms and with further simplification in (8):

$$u_j = u_i - 2(r_{ij}P_{ij} + x_{ij}Q_{ij}) + (r_{ij}^2 + x_{ij}^2)l_{ij} \quad (9)$$

With the angle relaxation and new-defined variables, the apparent power balance relationship from (3) at the bus $j$ is:

$$s_j^g - s_j^d = \sum_{k:j\rightarrow k} S_{jk} - \sum_{i:i\rightarrow j}(S_{ij} - z_{ij}l_{ij}) + y_ju_j \quad (10)$$

Splitting the (10) in terms of real and reactive power, the power balance at bus $j \in \mathcal{N}$ is as follows:

$$P_j^g - P_j^d = \sum_{k:j\rightarrow k} P_{jk} - \sum_{i:i\rightarrow j}(P_{ij} - r_{ij}l_{ij}) + g_ju_j \quad (11)$$

$$Q_j^g - Q_j^d = \sum_{k:j\rightarrow k} Q_{jk} - \sum_{i:i\rightarrow j}(Q_{ij} - x_{ij}l_{ij}) + b_ju_j \quad (12)$$

where $z_{ij} = r_{ij} + jx_{ij}$; $r_{ij}$ and $x_{ij}$ are the resistance and reactance of the line $L_{ij} \in \mathcal{L}$ respectively. $S_{ij} = P_{ij} + jQ_{ij}$, $y_j = g_j + jb_j$, $S_j^g = P_j^g + jQ_j^g$, and $S_j^d = P_j^d + jQ_j^d$.

*2) Conic Relaxation:* For each of the branches in the network, the OPF model is still non-convex due to the quadratic equation in (7) as:

$$l_{ij} = \frac{S_{ij}^2}{u_i} \Rightarrow l_{ij} = \frac{P_{ij}^2 + Q_{ij}^2}{u_i} \quad (13)$$

With the conic-relaxation, the non-convex solution space is enclosed within a feasible conic convex space [33]. For the proposed model, further convexification is done by conic relaxation in (13) with a conic inequality as follows in (14):

$$u_i + l_{ij} \geq \left\| \begin{matrix} 2P_{ij} \\ 2Q_{ij} \\ u_i - l_{ij} \end{matrix} \right\|_2 \quad (14)$$

Fig. 2(a) represents the conic space for the OPF solution. The solution gap is minimum if the OPF solution is on the surface and the gap increases if it moves away from the surface which is demonstrated in Fig.3. The difference between solution points A and B is the solution gap of the SOCP-OPF analysis.

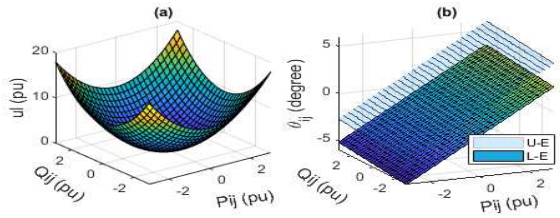


Fig. 2. (a) Representation of the conic space and (b) the envelope for $\theta_{ij}$, where U-E indicates upper level and L-E indicates lower level of the envelope.

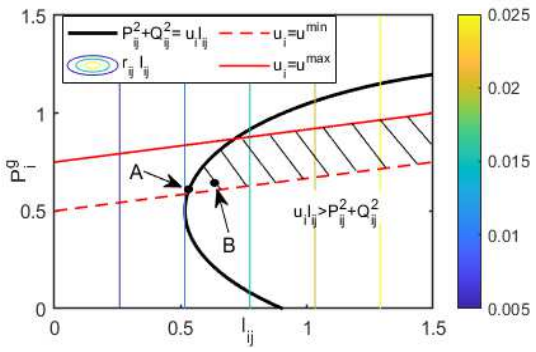


Fig. 3. Feasible zone: NLP vs. SOCP. The feasible space for the NLP lies at the boundary of the $P_{ij}^2 + Q_{ij}^2 = u_il_{ij}$ curve, while the feasible space for the SOCP is the shaded area right of the curve. Solution gap, $\sigma = |B - A|$.

*3) Cyclic Constraints:* It is stated in the earlier discussion that for an exact SOCP-OPF analysis, cyclic constraints need to be satisfied for mesh networks as shown below in (15):

$$\sum_{(i,j,\ldots x)\in\mathcal{C}} \theta_{ij} + \theta_{jk} + \ldots + \theta_{xi} = 0 \quad (15)$$

where suffixes $i$, $j$, and $x$ are the buses engaged with a particular mesh cycle ($\mathcal{C}$) in a power network. In the proposed OPF model, the bus voltage angle difference is retrieved based on (6), and the cyclic constraints in (15) are satisfied within the

convex solution space. For this purpose, (6) is relaxed within an envelope comprising (16) and (17) as boundary conditions.

$$\theta_{ij} \geq \frac{M}{\overline{V}_i \overline{V}_j \cos\frac{\theta_{ij}^m}{2}} - \tan\frac{\theta_{ij}^m}{2} + \frac{\theta_{ij}^m}{2} \tag{16}$$

$$\theta_{ij} \leq \frac{M}{\underline{V}_i \underline{V}_j \cos\frac{\theta_{ij}^m}{2}} + \tan\frac{\theta_{ij}^m}{2} - \frac{\theta_{ij}^m}{2} \tag{17}$$

where $M = V_i V_j \sin(\theta_{ij}) = \frac{B_{ij}P_{ij} - G_{ij}Q_{ij}}{G_{ij}^2 + B_{ij}^2}$. A visual representation of the proposed envelope is illustrated in Fig. 2 (b), and the derivation of the envelope is shown in Appendix A.

### C. Proposed SOCP-OPF Architecture

The primary goal of an OPF analysis is to provide a supply-demand balance based on an objective while satisfying the imposed network constraints. The proposed OPF model can be applied with different objective functions $f(x)$, such as network loss minimization, generation cost minimization, bus voltage regulation, or a combination of these. We have considered only convex objective functions for the proposed SOCP-OPF model in this article. The following objective functions are analyzed with the proposed OPF model.

a) Network power loss minimization:

$$min \sum_{L_{ij} \in \mathcal{L}} r_{ij} |I_{ij}|^2 \Rightarrow min \sum_{L_{ij} \in \mathcal{L}} r_{ij} l_{ij} \tag{18}$$

b) Real power generation cost minimization:

$$min \sum_{i \in \mathcal{N}_g} [c_2^i (P_i^g)^2 + c_1^i P_i^g + c_0^i] \tag{19}$$

where $c_2^i(\$/MWh^2)$, $c_1^i(\$/MWh)$ and $c_0^i(\$/h)$ represent the quadratic cost coefficients of the generator at the bus $i \in \mathcal{N}_g$. For considering the cost function as a convex equation $c^i \geq 0$. Finally, the proposed SOCP-OPF model with a convex objective function is as follows:

$$min \sum f(x_i) \tag{20}$$

Subject to: (9), (11), (12) and (14)- (17); along with the following imposed constraints on the control variables:

$$\begin{cases} \underline{P}_i^g \leq P_i^g \leq \overline{P}_i^g \\ \underline{Q}_i^g \leq Q_i^g \leq \overline{Q}_i^g \\ l_{ij} \leq \bar{l}_{ij} \\ \underline{u}_i \leq u_i \leq \overline{u}_i \end{cases} \tag{21}$$

where $P_i^g$ and $Q_i^g$ are the real and reactive power generation of the generator at the bus $i \in \mathcal{N}_g$. Voltage limits are defined as, $\underline{u}_i = |\underline{V}_i|^2$ and $\overline{u}_i = |\overline{V}_i|^2$ for the bus $i \in \mathcal{N}$. Current flow limit is defined as $\bar{l}_{ij} = |\overline{I}_{ij}|^2$. $\overline{I}_{ij}$ is the rated current flow limit for the branch $L_{ij} \in \mathcal{L}$.

### D. Graph Theory-Based Mesh Cycle Extraction

The proposed OPF analysis process starts with determining all the mesh cycles in a network. A graph theory-based methodology is proposed to find all the mesh cycles. The mesh cycles are determined from a network ex-ante of the SOCP-OPF analysis. The bus voltage angle difference between the buses is determined within the envelope defined by (16) & (17), which satisfies the cyclic angle constraints in the network with the imposed (15). An Adjacency matrix ($\mathcal{A}$) is generated for the network branches to find the cycles. If the bus number in a network is "$N_b$", then the size of the Adjacency matrix is $(N_b \times N_b)$. Graph vertices label the rows and columns of the matrix. If bus $i \in \mathcal{N}$ and bus $j \in \mathcal{N}$ are adjacent connected, then in position $(i, j)$ of $\mathcal{A}$ is 1 otherwise 0. Then with the interconnected branches, mesh cycles are traced. The shortest mesh cycle is considered for the model if a branch engages with multiple mesh cycles. The shortest mesh cycle has the least number of edges and buses engaged with the mesh. For example as shown in Fig. 6, the branch $L_{12}$ is engaged with multiple mesh cycles as $MC_1(1, 2, 5, 1)$, $MC_2(1, 2, 4, 5, 1)$ and $MC_3(1, 2, 3, 4, 5, 1)$. However, the mesh cycle $MC_1$ is considered the shortest for the branch $L_{12}$. If a branch $L_{ij}$ is already within a previous mesh cycle, then it does not need to find for another cycle. This approach is continued until all branches' mesh cycles are determined. If a network branch is not engaged with any mesh cycles, then that is listed as a dangling branch. The algorithm for the cycle extraction is illustrated in Algorithm 1. Worth to note that, in the meshed branches, power transmission networks usually have a few dangling branches forming a radial-type network part. For those radial type branches, the phase angle difference depends on the width of the envelopes derived in (16) and (17). If a tight envelope is considered with a smaller $\theta_{ij}^m$ (i.e., $10^o - 20^o$), the phase angle difference $(\theta_{ij})$ is retrieved during the OPF execution. However, if a broader range of $\theta_{ij}^m$ is considered for the envelope, $\theta_{ij}$ is recovered after the optimization process from (6). Algorithm 1 is also used to determine the radial-type dangling branches of the network. The execution time of Algorithm 1 for different test cases is shown in Table VII. Information regarding the cycles is included as a parameter in the proposed SOCP-OPF model after completing the mesh cycle extracting process before the optimization begins.

## III. Line Flow Limits and Bi-directional Flow

### A. Impact of Line Flow Limits

This section discusses the impact of the line flow limits on the SDP-OPF models compared to the proposed SOCP-OPF model. The SDP-OPF models fail to determine a feasible and physically meaningful solution for a tighter line-flow limit [28], [30]. To evaluate the impact of line flow limits on SDP, consider the power flow representation as follows:

$$P_i^g - P_i^d = \sum_{(i,j) \in \mathcal{N}} Re\{(W_{ii} - W_{ij}) y_{ij}^*\} \tag{22}$$

$$Q_i^g - Q_i^d = \sum_{(i,j) \in \mathcal{N}} Im\{(W_{ii} - W_{ij}) y_{ij}^*\} \tag{23}$$

**Algorithm 1:** Network Mesh Cycle Extraction

Determine the total bus number $N_b$ and branch number $N_L$ in the power network.
Get data input for "from bus $(f_b)$" and "to bus $(t_b)$", $\{f_b, t_b\} \in \mathcal{N}$ and form the Adjacency matrix $(\mathcal{A})$ of size $(N_b \times N_b)$.
Define a matrix **A** for the vertices engaged with mesh cycles in the network.
Define a matrix **B** for the vertices of the dangling branches.
**for** $n = 1 : N_L$ **do**
  **if** *branch* $L_{ij}(n)$ *is not already in matrix "**A**" or "**B**"* **then**
    Trace for the inter-connected branches from the branch $L_{ij}(n)$ for any mesh cycles $(\mathcal{C})$ engaged with $L_{ij}(n)$.
    **if** *branch* $L_{ij}(n)$ *is in '$k$' number of mesh cycles:* **then**
      Find the total number of buses in each mesh cycle from $\mathcal{C}_k$.
      Find the shortest path mesh cycle $\mathcal{C}_k^{shortest}$ engaged with the branch $L_{ij}(n)$ from $\mathcal{C}_k$.
      Find the total bus no. $N_{ij}^{mesh}$ in the shortest mesh cycle $\mathcal{C}_k^{shortest}$.
      **for** $m = 1$ *to* $N_{ij}^{mesh}$ **do**
        Find all of the bus indexes $i, j..x$ of the mesh cycle $\mathcal{C}_k^{shortest}$ and store them in the matrix **A**.
      **end**
    **end**
    **else if** *branch* $L_{ij}(n)$ *is not in a mesh* **then**
      Store the bus indexes $i$ & $j$ engaged with the dangling branch $L_{ij}$ in the matrix **B**.
    **end**
  **end**
**end**
The matrix **A** returns the cycles, and the matrix **B** returns the radial branches of the network.
Here, $\mathcal{C}_k^{shortest}$ is the shortest mesh cycle among the mesh cycles $\mathcal{C}_k$ for branch $L_{ij}$ with minimum edges.

where $W_{ii} = V_i V_i^*$ and $W_{ij} = V_i V_j^*$. $V_i$ and $V_j$ are the bus voltage at the bus $i \in \mathcal{N}$ and bus $j \in \mathcal{N}$ respectively. The inequality constraints are defined as follows:

$$\underline{P}_i^g \le P_i^g \le \overline{P}_i^g$$
$$\underline{Q}_i^g \le Q_i^g \le \overline{Q}_i^g$$
$$\underline{V}_i^2 \le W_{ii} \le \overline{V}_i^2$$

For a branch $L_{ij} \in \mathcal{L}$ connecting the buses $i \in \mathcal{N}$ and $j \in \mathcal{N}$, the line constraints can be imposed in a convex form as:

$$|S_{ij}| = |(W_{ii} - W_{ij}) y_{ij}^*| \le \overline{S}_{ij} \tag{24}$$

Splitting (24) in terms of real and reactive flow, the power flow relation can be represented as follows:

$$|P_{ij}| = |Real[|(W_{ii} - W_{ij}) y_{ij}^*|]| \le \overline{P}_{ij} \tag{25}$$

$$|Q_{ij}| = |Imag[|(W_{ii} - W_{ij}) y_{ij}^*|]| \le \overline{Q}_{ij} \tag{26}$$

where $W \in \boldsymbol{H}^n$ is a semidefinite Hermitian matrix. The SDP-OPF formulation is tight and the solution is feasible optimal if $W \ge 0$ and $rank\{W\} = 1$.

**Remark 1.** *If a narrow band line flow limits are imposed on (24), then the SDP-OPF solver computationally fails or leads to an incorrect solution.*

*Proof.* From (24) it can be written as, $|(W_{ii} - W_{ij}) y_{ij}^*| \le \overline{S}_{ij} \Rightarrow |(V_i V_i^* - V_i V_j^*) y_{ij}^*| \le \overline{S}_{ij}$. If $i \in \mathcal{N}$ and $j \in \mathcal{N}$ are two adjacent buses connected with a line $L_{ij} \in \mathcal{L}$; $V_i = V_m \angle \theta$; $V_j = (V_m + \Delta V) \angle (\theta + \Delta\theta)$ and $y_{ij} = \frac{1}{z_{ij} \angle \theta_{ij}}$, then

$$|\{V_m^2 - (V_m^2 + V_m \Delta V) \angle -\Delta\theta\} y_{ij}^*| \le \overline{S}_{ij} \tag{27}$$

If the SDP OPF is characterized with a voltage range $[1 - \xi, 1 + \xi]$, where $\xi$ is small, then $-2\xi \le \Delta V \le 2\xi$. Thus $V_m \Delta V \approx 0$ or negligible $\Rightarrow |(V_m^2 - V_m^2 \angle -\Delta\theta) y_{ij}^*| \le \overline{S}_{ij}$. This means $|V_m^2 (1 - 1\angle -\Delta\theta)| y_{ij} | \angle \delta_{ij}| \le \overline{S}_{ij}$. Then in terms of real power, it can be shown that:

$$|V_m^2 |y_{ij}| \{\cos \delta_{ij} - \cos(\delta_{ij} - \Delta\theta)\}| \le \overline{P}_{ij} \tag{28}$$

For a branch $L_{ij} \in \mathcal{L}$ the line impedance is $z_{ij} = r_{ij} + j x_{ij}$. Considering that for a transmission network, $x_{ij} >> r_{ij}$ and $y_{ij} = \frac{1}{z_{ij} \angle \delta_{ij}}$; $\delta_{ij} \approx \frac{\pi}{2}$. So for a transmission network (28) can be represented as follows:

$$||y_{ij}| V_m^2 \sin(\Delta\theta)| \le \overline{P}_{ij} \tag{29}$$

If the voltage phase angle difference $\Delta\theta$ between two adjacent connected buses is not significantly low, the lower line flow constraint shown in (29) fails. So, the solution from the SDP formulation becomes infeasible or inaccurate.

The SOCP-OPF model is relaxed with the conic relaxation as $u_i l_{ij} \ge S_{ij}^2$. The current flow $l_{ij} = |I_{ij}|^2$ is proportional to the apparent power flow $S_{ij}$. So, in contrast with the SDP-OPF models, the SOCP-OPF models do not suffer from the line flow limit issue. □

*1) Example:* The impact of the line flow limit on the SOCP-OPF and SDP-OPF analysis is illustrated with an example of the IEEE 5-bus network [34], shown in Fig. 4. Line flow

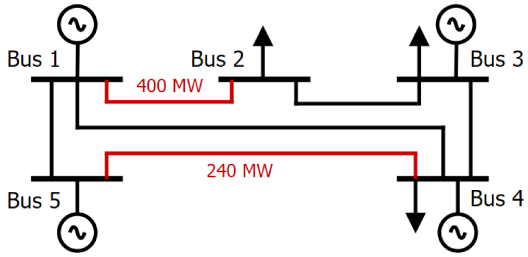


Fig. 4. Schematic diagram of the IEEE 5-bus network (Ref: MATPOWER).

limits are imposed on the two branches $L_{1,2}$ and $L_{4,5}$, as $\overline{P}_{(1,2)} = 400MW$ and $\overline{P}_{(4,5)} = 240MW$ respectively. It is observed that the SDP-OPF model became infeasible with these network constraints. Further, the two-line flow limits have been increased by a multiplying factor $\epsilon$. For a range of

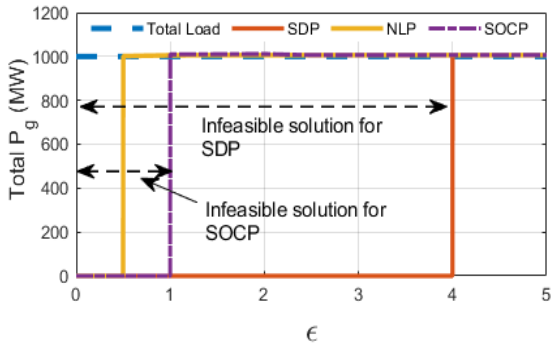


Fig. 5. Impact of the branch flow limits on different OPF models.

$\epsilon\overline{P}_{(1,2)}$ and $\epsilon\overline{P}_{(4,5)}$; the network has been solved with different OPF models, and the results are illustrated in Fig. 5. With the increase of the value of $\epsilon$, the line limit increases (i.e., when $\epsilon = 2$, the flow limit is increased by $100\%$). The total load is 1000 MW in the network, and a feasible solution occurs when the total generation meets the total demand. Besides the IEEE 5-bus network, tighter line limits are also imposed and tested for different branches in the IEEE 57 and 118-bus networks. Because of the stricter line limits, the SDP-OPF model computationally fails to provide a feasible solution as opposed to the SOCP-OPF model.

### *B. Bi-directional Flow in SOCP-OPF*

The SOCP-based OPF models are widely used for radial-type power networks, and the conditions for the exact solution for any reverse power flow are discussed in [35]. However, it is necessary to check the feasibility of the SOCP-OPF model for possible bi-directional power flow conditions for meshed network systems. Consider bus $j \in \mathcal{N}$ in Fig. 1 with connected two adjacent buses $i \in \mathcal{N}$ & $k \in \mathcal{N}$. The power flow through the branches connected with the bus $j \in \mathcal{N}$ is as follows:

$$\begin{aligned} P_{ij} &= r_{ij}l_{ij} - P_{ji} \\ P_{jk} &= r_{jk}l_{jk} - P_{kj} \\ P_{lj} &= r_{lj}l_{lj} - P_{jl} \\ P_{jm} &= r_{jm}l_{jm} - P_{mj} \end{aligned} \tag{30}$$

These relations can be derived for reactive power flow as well. From Fig. 1, the real power balance at the bus $j \in \mathcal{N}$ is as:

$$P_j^g - P_j^d = \sum_{k:j\rightarrow k} P_{jk} - \sum_{i:i\rightarrow j} (P_{ij} - r_{ij}l_{ij}) + g_j u_j \tag{31}$$

If the power flows in at bus $j$ from the bus $i$ and $l$ and goes out to the bus $k$ and $m$ then from (31):

$$P_j^g - P_j^d = P_{jk} + P_{jm} - (P_{ij} - r_{ij}l_{ij}) - (P_{lj} - r_{lj}l_{lj}) \tag{32}$$

If the direction of power flow at bus $j$ is reversed, then:

$$P_j^g - P_j^d = P_{jl} + P_{ji} - (P_{kj} - r_{kj}l_{kj}) - (P_{mj} - r_{mj}l_{mj}) \tag{33}$$

From (32) and (33); $l_{jk} = l_{kj}$ and $l_{jm} = l_{mj}$. If the solution gap from the proposed SOCP model is minimal for the forward flow from bus $i$ to bus $j$, then $S_{ij}^2 \cong u_i l_{ij}$. If the power flows from bus $j$ to bus $i$, the solution will also be considered exact if it satisfies $S_{ji}^2 \cong u_j l_{ij}$, which can be extended as follows:

$$S_{ij}^2 + (r_{ij}^2 + x_{ij}^2)l_{ij}^2 - 2l_{ij}(P_{ij}r_{ij} - Q_{ij}x_{ij}) \cong u_j l_{ij} \tag{34}$$

As the optimal solution for the forward flow is considered with a minimal solution gap as $S_{ij}^2 \cong u_i l_{ij}$, then from (34):

$$(r_{ij}^2 + x_{ij}^2)l_{ij} - 2(P_{ij}r_{ij} - Q_{ij}x_{ij}) \cong 0 \tag{35}$$

For the proposed SOCP-OPF model the voltage relation between bus $i \in \mathcal{N}$ and bus $j \in \mathcal{N}$ is expressed as follows:

$$u_j = u_i - 2(r_{ij}P_{ij} + x_{ij}Q_{ij}) + (r_{ij}^2 + x_{ij}^2)l_{ij} \tag{36}$$

From (35) and (36) for a reverse flow, the solution gap is also minimal if $u_i \cong u_j$. For the reverse flow in the branch $L_{jk} \in \mathcal{L}$, it can also be shown that for minimal gap solution, $u_j \cong u_k$. Suppose there is any possible bi-directional flow through a branch in a mesh network; the OPF solution gap will be minimal if the bus voltage difference between the two connected buses with that particular branch is minimal.

## IV. Exactness and the Optimality of the Proposed SOCP-OPF Model

The exactness and the global optimality of the proposed SOCP-OPF model are discussed in this section. The feasible set of the OPF problem is convex with the angle relaxation and conic relaxation of the non-linear equality in (13) within a conic space. The exactness of an OPF solution from the proposed model depends on the conic space formed by (14) and the cyclic angle constraints. The solution gap is defined as, $\sigma = |u_i l_{ij} - S_{ij}^2|$ in this article.

For the proposed OPF model, we have considered the objective function $f(x)$ as convex and increasing with the current flow $I_{ij}$. Let us consider an optimal solution set from the proposed OPF model as, $\tilde{\psi} = (\tilde{S}_{ij}, \tilde{l}_{ij}, \tilde{u}, \tilde{S}_g)$. Further, assume there exist another feasible solution set as $\hat{\psi} = (\hat{S}_{ij}, \hat{l}_{ij}, \hat{u}, \hat{S}_g)$, where $\hat{l}_{ij} = \tilde{l}_{ij} - \epsilon$, $\hat{S}_{ij} = \tilde{S}_{ij} - \epsilon z_{ij}$, $\hat{u}_i = \tilde{u}_i$, $\hat{S}_i^g = \tilde{S}_i^g$, $\hat{S}_i^d = \tilde{S}_i^d + \epsilon z_{ij}$ and $\hat{S}_j^d = \tilde{S}_j^d$ for a $\epsilon \geq 0$. Also, the solution $\hat{\psi}$ satisfies the angle cyclic constraints. The OPF objective value $f(\hat{\psi})$ is smaller than the objective value $f(\tilde{\psi})$ as, $\hat{l}_{ij} = \tilde{l}_{ij} - \epsilon$, has a strict smaller value. This contradicts the optimality of the solution set $\tilde{\psi}$ from the proposed OPF model. The proposed model will be proved as tight, and the solution is globally optimal if the cyclic constraints are satisfied and there is no other solution set lower than $\tilde{\psi}$. It is sufficient to show $\epsilon = 0$ for proving the global optimality. The following remarks validate the global optimality and the tightness of the model when cyclic constraints are satisfied in a mesh network.

**Remark 2.** *An optimal solution set is within the conic convex solution space if the solution satisfies (9), (11), (12), and (14).*

*Proof.* As $\tilde{\psi}$ is the optimal solution from the proposed OPF model, it satisfies (9), (11), (12) and (14). The (11) and (12) are derived in terms of real and reactive power by splitting the (10). For analyzing (11)-(12) together, the power flow equation (10) with the apparent power $S_i^g$, apparent power flow $S_{ij}$, and

current flow $l_{ij}$ are considered here for the bus $i$ & $j \in \mathcal{N}$. For the solution set $\hat{\psi}$ at the bus $i \in \mathcal{N}$:

$$\begin{aligned}\hat{S}_i &= \hat{S}_i^g - \hat{S}_i^d = \tilde{S}_i^g - \tilde{S}_i^d - \epsilon z_{ij} \\ &= \sum_{j:i\rightarrow j} \tilde{S}_{ij} - \sum_{k:k\rightarrow i} (\tilde{S}_{ki} - z_{ki}\tilde{l}_{ki}) + y_i\tilde{u}_i - \epsilon z_{ij} \\ &= \sum_{j':i\rightarrow j', j\neq j'} \hat{S}_{ij'} + (\hat{S}_{ij} + \epsilon z_{ij}) - \sum_{k:k\rightarrow i} (\hat{S}_{ki} - z_{ki}\hat{l}_{ki}) \\ &\qquad + y_i\hat{u}_i - \epsilon z_{ij} \\ &= \sum_{j:i\rightarrow j} \hat{S}_{ij} - \sum_{k:k\rightarrow i} (\hat{S}_{ki} - z_{ki}\hat{l}_{ki}) + y_i\hat{u}_i\end{aligned}$$

At the bus $j \in \mathcal{N}$:

$$\begin{aligned}\hat{S}_j &= \hat{S}_j^g - \hat{S}_j^d = \tilde{S}_j^g - \tilde{S}_j^d \\ &= \sum_{k:j\rightarrow k} \tilde{S_{jk}} - \sum_{i:i\rightarrow j} (\tilde{S_{ij}} - z_{ij}\tilde{l_{ij}}) + y_j\tilde{u}_j \\ &= \sum_{k:j\rightarrow k} \hat{S_{jk}} - \sum_{i':i'\rightarrow j, i'\neq i} (\hat{S_{i'j}} - z_{i'j}\hat{l_{i'j}}) + y_j\hat{u}_j \\ &\qquad - [(\hat{S_{ij}} + \epsilon z_{ij}) - z_{ij}(\hat{l_{ij}} + \epsilon)] \\ &= \sum_{k:j\rightarrow k} \hat{S_{jk}} - \sum_{i:i\rightarrow j} (\hat{S_{ij}} - z_{ij}\hat{l_{ij}}) + y_j\hat{u}_j\end{aligned}$$

For the solution set $\tilde{\psi}$, the voltage relation (9) is as follows considering the branch $L_{ij} \in \mathcal{L}$:

$$\begin{aligned}&\tilde{u_j} = \tilde{u_i} - 2(r_{ij}\tilde{P}_{ij} + x_{ij}\tilde{Q}_{ij}) + (r_{ij}^2 + x_{ij}^2)\tilde{l}_{ij} \\ &\Rightarrow \hat{u_j} = \hat{u_i} - 2[r_{ij}(\hat{P}_{ij} + \epsilon r_{ij}) + x_{ij}(\hat{Q}_{ij} + \epsilon x_{ij})] \\ &\qquad + (r_{ij}^2 + x_{ij}^2)(\hat{l}_{ij} + \epsilon) \\ &\Rightarrow \hat{u_j} = \hat{u_i} - 2(r_{ij}\hat{P}_{ij} + x_{ij}\hat{Q}_{ij}) + (r_{ij}^2 + x_{ij}^2)\hat{l}_{ij} \\ &\qquad - \epsilon(r_{ij}^2 + x_{ij}^2)\end{aligned}$$

The solution $\hat{\psi}$ satisfies (9) if $\epsilon(r_{ij}^2 + x_{ij}^2) \approx 0$. As for a branch $L_{ij} \in \mathcal{L}$, $(r_{ij}^2 + x_{ij}^2) \neq 0$. So $\hat{\psi}$ satisfies (9) only if $\epsilon = 0$.

As, $\tilde{\psi}$ is the optimal solution from the proposed OPF model, it is within the conic space as follows:

$$\begin{aligned}&\tilde{u}_i\tilde{l}_{ij} - \tilde{S}_{ij}^2 \geq 0 \\ &\Rightarrow \hat{u_i}(\hat{l}_{ij} + \epsilon) - (\hat{S}_{ij} + z_{ij}\epsilon)^2 \geq 0 \\ &\Rightarrow \hat{u_i}\hat{l}_{ij} - \hat{S}_{ij}^2 + \epsilon[\hat{u}_i - z_{ij}^2\epsilon - 2\hat{S}_{ij}z_{ij}] \geq 0\end{aligned}$$

If $\epsilon = 0$; $\hat{u_i}\hat{l_{ij}} - \hat{S_{ij}^2} \geq 0$. The solution set $\hat{\psi}$ is within the conic space and the solution gap $\epsilon[\hat{u}_i - z_{ij}^2\epsilon - 2\hat{S}_{ij}z_{ij}]$ is minimal. □

**Remark 3.** *When the solution satisfies the cyclic angle constraints, the OPF model is tight, along with when $\epsilon = 0$ the solution from the proposed OPF model is globally optimal.*

*Proof.* $\hat{\psi}$ is the optimal solution with a minimal solution gap satisfying the cyclic angle constraints in the network. So for a mesh including the branch $L_{ij} \in \mathcal{L}$:

$$\sin^{-1}\frac{B_{ij}\hat{P}_{ij} + G_{ij}\hat{Q}_{ij}}{\hat{V}_i\hat{V}_j(G_{ij}^2 + B_{ij}^2)} + \sin^{-1}\frac{B_{jk}P_{jk} + G_{jk}Q_{jk}}{V_jV_k(G_{jk}^2 + B_{jk}^2)} + ... + \sin^{-1}\frac{B_{j'i}P_{j'i} + G_{j'i}Q_{j'i}}{V_{j'}V_i(G_{j'i}^2 + B_{j'i}^2)} = 0 \tag{37}$$

As the cyclic angle constraint is imposed on the proposed SOCP-OPF model for the solution $\tilde{\psi}$ in the mesh cycle consisting of the branch $L_{ij} \in \mathcal{L}$. Then for the solution set of $\tilde{\psi}$:

$$\begin{aligned}&\sin^{-1}\frac{B_{ij}\tilde{P}_{ij} + G_{ij}\tilde{Q}_{ij}}{\tilde{V}_i\tilde{V}_j(G_{ij}^2 + B_{ij}^2)} + \sin^{-1}\frac{B_{jk}P_{jk} + G_{jk}Q_{jk}}{V_jV_k(G_{jk}^2 + B_{jk}^2)} + ... + \sin^{-1}\frac{B_{j'i}P_{j'i} + G_{j'i}Q_{j'i}}{V_{j'}V_i(G_{j'i}^2 + B_{j'i}^2)} = 0 \\ &\Rightarrow \sin^{-1}\frac{B_{ij}\hat{P}_{ij} + G_{ij}\hat{Q}_{ij} + \epsilon(B_{ij}r_{ij} + G_{ij}x_{ij})}{\hat{V}_i\hat{V}_j(G_{ij}^2 + B_{ij}^2)} + \sin^{-1}\frac{B_{jk}P_{jk} + G_{jk}Q_{jk}}{V_jV_k(G_{jk}^2 + B_{jk}^2)} + ..... \\ &\qquad + \sin^{-1}\frac{B_{j'i}P_{j'i} + G_{j'i}Q_{j'i}}{V_{j'}V_i(G_{j'i}^2 + B_{j'i}^2)} = 0\end{aligned} \tag{38}$$

$\hat{\psi}$ is the optimal solution with a minimal solution gap. So, comparing (37) and (38) if $\epsilon \approx 0$; the cyclic constraints are satisfied similarly for $\tilde{\psi}$ as $\hat{\psi}$. The solution gap for $\tilde{\psi}$ is also minimal. The solution gap, defined as $\sigma = |u_il_{ij} - S_{ij}^2|$ is measured after the OPF analysis. The solution gap ($\sigma$) is very small from the proposed model for the test cases in this article.

Further, for the two solution set $\tilde{\psi}$ and $\hat{\psi}$, it is assumed $f(\hat{\psi}) \leq f(\tilde{\psi})$. From the definition of the convexity for convex objective functions:

$$f(a\hat{\psi} + (1-a)\tilde{\psi}) \leq af(\hat{\psi}) + (1-a)f(\tilde{\psi}) \tag{39}$$

where $a \in [0, 1]$. Then:

$$\begin{aligned}&af(\hat{\psi}) + (1-a)f(\tilde{\psi}) \leq af(\tilde{\psi}) + (1-a)f(\tilde{\psi}) \\ &\Rightarrow af(\hat{\psi}) + (1-a)f(\tilde{\psi}) \leq f(\tilde{\psi})\end{aligned} \tag{40}$$

From (39) and (40):

$$f(a\hat{\psi} + (1-a)\tilde{\psi}) \leq f(\tilde{\psi}) \tag{41}$$

Since $f(\tilde{\psi})$ is the optimal solution, so for any other solution within the convex space is $f(\psi) > f(\tilde{\psi})$, which contradicts with (41). To satisfy both conditions it must be $\tilde{\psi} = \hat{\psi}$, thus $\epsilon = 0$. So for a convex objective function, it is impossible to have another solution set lower than $\tilde{\psi}$. So the solution from the proposed OPF model is globally optimal and satisfies the cyclic angle constraints in the mesh network. □

## V. Simulation Results and Discussions

The proposed OPF model has been simulated and tested in the MATLAB® with the MOSEK® solver platform. The proposed OPF model is simulated in multiple standard test cases (i.e., IEEE 14-bus, 57-bus, 118-bus, and 2736-bus network systems [34]) and a synthetic 500-bus network [36]. The results from the proposed SOCP-OPF model are compared with the NLP-OPF and SDP-OPF solutions from MATPOWER® [34]. The solution from the SDP-OPF in MATPOWER® for the 118-bus network is globally optimal and feasible with a minimum branch resistance of $1 \times 10^{-4}$ per unit [27]. Thus, The same network conditions are applied in the proposed SOCP-OPF model. It has been observed that the solution from the SOCP-OPF model matches with the solution from the SDP-OPF proven to yield global optimal solutions [27] for the test systems considered.

### A. Implementation of the Proposed SOCP-OPF Model

The model implementation starts with the identification of the mesh cycles in the network using Algorithm 1. Then the optimization process is executed with the proposed SOCP-OPF model, where the cyclic constraints for all the meshes are

satisfied. This improves the exactness of the SOCP-OPF model for mesh networks and provides a globally optimal solution.

As an illustrative example, in Fig. 6, the schematic diagram of the IEEE 14-bus network shows the mesh cycles with all of the branches associated with any loop. In the network, bus no. 8 is not associated with any mesh cycle and is considered as a radial type dangling branch from the Algorithm 1. Table

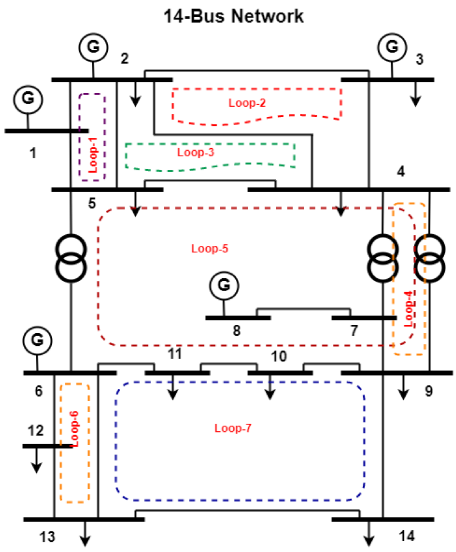


Fig. 6. Single line schematic diagram of the IEEE 14-bus network.

Table I
COMPARISON OF THE ANGLE DIFFERENCE SUMMATION OVER CYCLES BETWEEN SOCP WITH CYCLIC CONSTRAINTS (CC) AND WITHOUT CYCLIC CONSTRAINTS (WCC) ON THE IEEE 14-BUS NETWORK

| Loop No. | SOCP-WCC 100% load (Degree) | SOCP-CC 100% load (Degree) | SOCP-WCC 200% load (Degree) | SOCP-CC 200% load (Degree) |
|---|---|---|---|---|
| 1 | 2.1347 | 3.803e-07 | 4.4935 | 1.007e-06 |
| 2 | -2.9525 | 0 | -4.9639 | 0 |
| 3 | 0.0272 | 1.493e-07 | -0.5300 | 6.981e-08 |
| 4 | -0.3881 | 0 | -2.2302 | 0 |
| 5 | -0.5042 | -9.94e-17 | 1.7143 | 1.988e-16 |
| 6 | 0.0999 | 0 | 0.8921 | 0 |
| 7 | -0.1146 | 0 | -0.394 | 0 |

I shows the comparison of the bus voltage phase difference summation over mesh cycles between SOCP-OPF with cyclic constraints (CC) and without cyclic constraints (WCC) for different loading conditions. For the WCC, the sum of the angle difference increases with the higher loading conditions. As a convex OPF model, the proposed model promises a globally optimal solution for convex objectives with the imposed cyclic constraints. The OPF solution from the proposed model for the IEEE 14-bus network is compared with the benchmark results from NLP-OPF and SDP-OPF models in MATPOWER. The real and reactive power generation for the minimum generation cost objective function is shown in Table II and Table III. It is observed that the power generation in different buses is the same as the NLP-OPF model from MATPOWER.

The proposed OPF model is further simulated on more extensive networks to check the scalability. Table. IV shows

Table II
GENERATION COMPARISON IN IEEE 14-BUS NETWORK (LINEAR COST FUNCTION)

| Bus No. | $C_1$ | Pg (MW) (SOCP) | Qg (MVAR) (SOCP) | Pg (MW) (NLP) | Qg (MVAR) (NLP) |
|---|---|---|---|---|---|
| 1 | 20 | 128.58 | 0 | 128.58 | 0 |
| 2 | 20 | 139.99 | 21.72 | 140.00 | 21.70 |
| 3 | 40 | 0 | 30.04 | 0 | 30.04 |
| 6 | 40 | 0 | 10.22 | 0 | 10.15 |
| 8 | 40 | 0 | 8.05 | 0 | 8.05 |

Table III
GENERATION COMPARISON IN IEEE 14-BUS NETWORK (QUADRATIC COST FUNCTION)

| Bus No. | $C_2$ | $C_1$ | $C_0$ | Pg (MW) (SOCP) | Qg (MVAR) (SOCP) | Pg (MW) (NLP) | Qg (MVAR) (NLP) |
|---|---|---|---|---|---|---|---|
| 1 | 0.04 | 20 | 0 | 194.40 | 0 | 194.43 | 0 |
| 2 | 0.25 | 20 | 0 | 36.78 | 23.70 | 36.80 | 23.67 |
| 3 | 0.01 | 40 | 0 | 28.74 | 25.12 | 28.75 | 25.13 |
| 6 | 0.01 | 40 | 0 | 0 | 12.71 | 0 | 12.63 |
| 8 | 0.01 | 40 | 0 | 8.52 | 8.51 | 8.50 | 8.51 |

the generation comparisons of the proposed SOCP-OPF model with NLP-OPF and a convex SDP-OPF model. The network conditions for the proposed SOCP-OPF model are the same as the MATPOWER models. The percent of generation mismatch between the proposed SOCP-OPF vs. NLP-OPF and SOCP-OPF vs. SDP-OPF model is illustrated in Table IV. MATPOWER uses an interior point solver. Due to the solver difference, there is a negligible generation discrepancy between the OPF models. The maximum real power difference for the SOCP-OPF vs. NLP-OPF is 0.09% (2736-Bus Network), and the reactive power difference is 0.84% (118-Bus Network). For the SOCP-OPF vs. SDP-OPF, the maximum real power difference is 0.11%, and the reactive power difference is 0.81% (2736-Bus Network). Due to space constraints, only the voltage profile of the IEEE 118-bus network is demonstrated in Fig.7. The power loss from the proposed SOCP-OPF model and the voltage profile mismatch between the proposed OPF model and the NLP-OPF model is illustrated in Table VI. The tightness of the OPF model has been analyzed using the solution gap from (14) represented as $\sigma = |u_i l_{ij} - S_{ij}^2|$. The solution gap ($\sigma$) for all the branches is measured, and the average value is presented in Table VI. For all of the test cases, the $\sigma$ and % of voltage deviation ($\Delta v$) are minimal for the proposed OPF model compared to the NLP counterpart. The convergence time of the proposed SOCP-OPF is compared with the SDP-OPF and NLP-OPF models as shown in Table VII. The test system is an Intel(R) Core(TM) i7-10510U CPU, 2.30 GHz processor, and 16 GB RAM machine. From the results shown in Table VII, it is observed that the convergence time for the proposed SOCP-OPF model is significantly lower than the NLP-OPF and SDP-OPF models.

### *B. Impact of the Envelope Width on the SOCP-OPF*

This section evaluates one of the major contributions to deriving a convex envelope based on (16) and (17). The optimal solution from the proposed model includes an optimal

Table IV
COMPARISON OF DIFFERENT OPF MODELS WITH THE PROPOSED SOCP-OPF MODEL

| Test Case | Connected Load | | SOCP | | NLP | | SDP | | SOCP vs NLP | | SOCP vs SDP | |
|---|---|---|---|---|---|---|---|---|---|---|---|---|
| | Pd (MW) | Qd (MVAR) | Pg (MW) | Qg (MVAR) | Pg (MW) | Qg (MVAR) | Pg (MW) | Qg (MVAR) | $\Delta P_g$ | $\Delta Q_g$ | $\Delta P_g$ | $\Delta Q_g$ |
| 14-Bus Network | 259.00 | 73.50 | 268.44 | 70.44 | 268.58 | 69.94 | 268.58 | 69.94 | 0.05% | 0.70% | 0.05% | 0.70% |
| 57-Bus Network | 1250.80 | 336.40 | 1266.61 | 273.60 | 1267.00 | 272.24 | 1267.00 | 272.24 | 0.03% | 0.50% | 0.03% | 0.50% |
| 118-Bus Network | 4242.00 | 1438.00 | 4328.47 | 455.67 | 4329.05 | 451.84 | 4329.05 | 457.73 | 0.01% | 0.84% | 0.01% | 0.45% |
| 500-Bus Network | 3692.69 | 984.73 | 3750.68 | 608.31 | 3750.43 | 607.40 | 3750.41 | 607.58 | .006% | 0.15% | .007% | 0.12% |
| 2736-Bus Network | 18074.5 | 5837.2 | 18419.3 | 3042.4 | 18437.4 | 3056.5 | 18439.7 | 3067.2 | 0.09% | 0.46% | 0.11% | 0.81% |

Table V
IMPACT OF THE WIDTH OF THE PROPOSED ENVELOPE ON THE $\theta_{ij}$ FROM THE PROPOSED SOCP-OPF MODEL

| Test Case | $\theta_{ij}^m$ (Degree) | Branch No. with Maximum $\theta_{ij}$ | Connected Buses (From-To) | Envelope Lower Limit (Degree) | Envelope Upper Limit (Degree) | $\theta_{ij}$ From the Model (Degree) | Standard Deviation $\Delta\theta_{ij}$ (Degree) |
|---|---|---|---|---|---|---|---|
| 14-Bus Network | 20° | 3 | 2-3 | 8.6447 | 8.9503 | 8.6562 | 0.2969 |
| | 30° | 3 | 2-3 | 8.5482 | 9.6529 | 8.8552 | 0.3951 |
| 57-Bus Network | 20° | 8 | 8-9 | 5.1142 | 5.4198 | 5.1611 | 0.1330 |
| | 30° | 8 | 8-9 | 5.0916 | 5.7963 | 5.2189 | 0.2487 |
| 118-Bus Network | 20° | 68 | 49-42 | 18.575 | 18.781 | 18.594 | 0.3507 |
| | 30° | 68 | 49-42 | 18.086 | 18.791 | 18.607 | 0.4451 |
| 500-Bus Network | 20° | 521 | 247-246 | 14.580 | 14.620 | 14.591 | 0.2061 |
| | 30° | 521 | 247-246 | 14.570 | 14.621 | 14.593 | 0.3472 |
| 2736-Bus Network | 20° | 74 | 28-25 | 12.087 | 12.292 | 12.170 | 0.2601 |
| | 30° | 74 | 28-25 | 12.076 | 12.781 | 12.657 | 0.3670 |

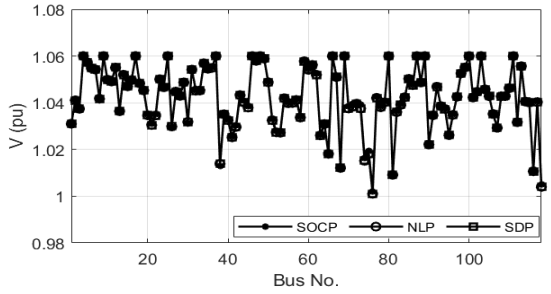


Fig. 7. Voltage profile for the IEEE 118-bus network.

Table VI
VOLTAGE COMPARISON BETWEEN SOCP-OPF VS NLP-OPF

| Test case | Voltage Mismatch (SOCP vs NLP) | Power Loss (SOCP) | Avg. Solution Gap (SOCP) |
|---|---|---|---|
| 14-Bus Network | 0.000 % | 3.56 % | 5.1e-09 |
| 57 Bus Network | 0.008 % | 1.28 % | 9.4e-09 |
| 118-Bus Network | 0.015 % | 1.99 % | 2.3e-09 |
| 500-Bus Network | 0.007 % | 1.54 % | 1.4e-08 |
| 2736-Bus Network | 0.025 % | 1.87 % | 7.03e-09 |

bus voltage angle difference within the envelope based on the power flow and satisfies the cyclic angle constraints as (15). The impact of the envelope width on the $\theta_{ij}$ is illustrated in Fig. 8 for the IEEE 14-bus, IEEE 57-bus, and IEEE 118-bus networks. In the figure, $\theta_{ij}$ is shown for the $\theta_{ij}^m = 20°$, and 30°, where, $\theta_{ij}^m$ is defined as $\theta_{ij}^m = max[|\underline{\theta_{ij}}|, |\overline{\theta_{ij}}|]$ for the envelope in (16) and (17). While $\theta_{ij}^m$ increases, the width of the envelope increases, so the deviation of $\theta_{ij}$ from the optimal point increases, which is illustrated in Table V. The $\theta_{ij}(NLP)$ is the reference value determined from the NLP-OPF solution in MATPOWER. Then the standard deviation of $\theta_{ij}$ is illustrated as $\Delta\theta_{ij}$, which is defined as $\Delta\theta_{ij} = \sqrt{\frac{[\theta_{ij}(NLP)-\theta_{ij}(SOCP)]^2}{N_L}}$, $N_L$ is the total number of branches in the network. From the analysis, the standard deviations are considerably low even for $\theta_{ij}^m = 30^o$ for all the cases, which is an acceptable range for the envelope for most practical transmission networks. From this, it is observed that a reasonable width can be considered for the envelope with the proposed SOCP-OPF model for optimal operation. The impact of the envelope width on the solution gap ($\sigma$) is illustrated in Fig. 9 for the IEEE 118-bus network. It is observed as when the width of the envelope is smaller, and the cyclic constraints (CC) are considered, the solution gap ($\sigma$) is considerably lower than without considering (WCC). With the cyclic constraints, the solution gap ($\sigma$) is less than $1 \times 10^{-7}$. The figure shows the results in per-unit (pu) with a base of 100 MVA. This concludes that the proposed model's cyclic constraints significantly improve the exactness of the SOCP-OPF model for mesh networks.

Table VII
OPF SOLUTION CONVERGENCE TIME COMPARISON AND EXECUTION TIME OF ALGORITHM 1

| Test Case | Run Time (sec) (Algorithm 1) | OPF Convergence Time (sec) | | |
|---|---|---|---|---|
| | | SOCP | NLP | SDP |
| 14-Bus Network | 0.34 | 0.31 | 0.34 | 0.39 |
| 57-Bus Network | 1.52 | 0.34 | 0.56 | 0.44 |
| 118-Bus Network | 2.04 | 0.41 | 0.64 | 0.48 |
| 500-Bus Network | 6.24 | 0.52 | 1.05 | 6.47 |
| 2736-Bus Network | 15.85 | 1.47 | 3.52 | 322.4 |

### C. Analysis of Voltage Difference on the Solution Gap

The effect of the voltage change for bi-directional flow is analyzed with the change of loading conditions. A load in a particular bus is changed with a multiplying factor $\lambda \in [0, 3]$

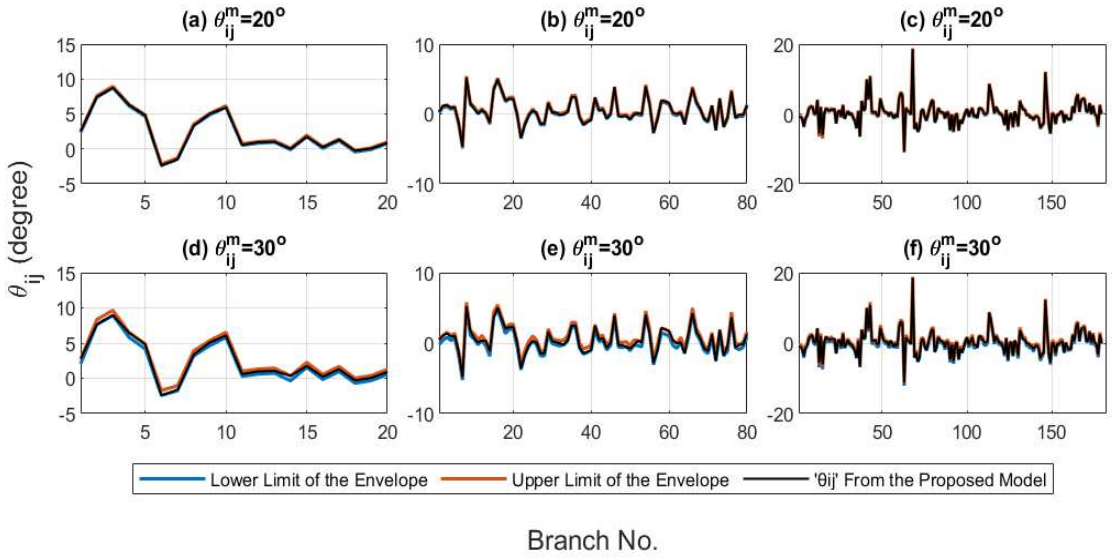


Fig. 8. $\theta_{ij}$ from the proposed envelope satisfying the cyclic constraints. Here, (a) & (d) are for the IEEE 14-bus network, (b) & (e) are for the IEEE 57-bus network, and (c) & (f) are for the IEEE 118-bus network, respectively.

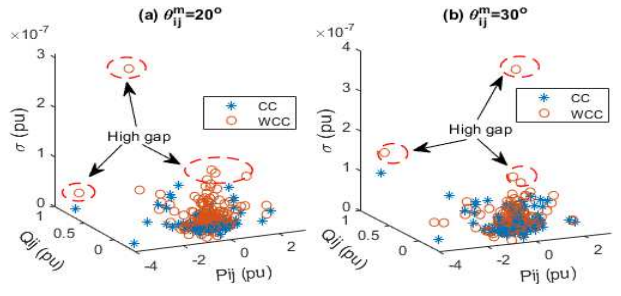


Fig. 9. Impact of the envelope width on the solution gap ($\sigma$) for the IEEE 118-bus network (a) $\theta_{ij}^m = 20^o$ (b) $\theta_{ij}^m = 30^o$.

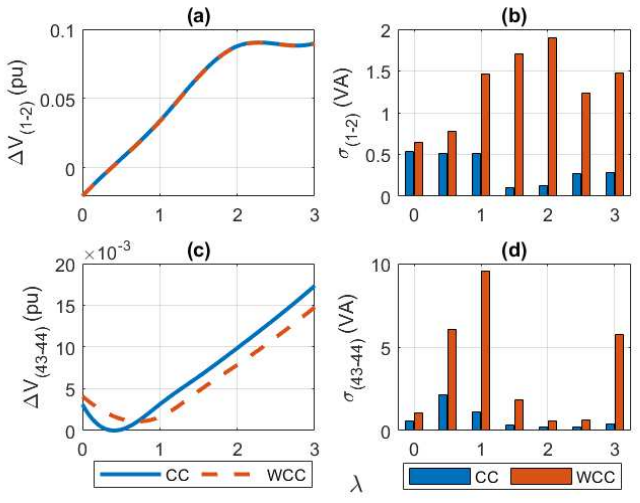


Fig. 10. Impact of the bus voltage difference on the solution gap ($\sigma$). Here, (a) & (b) and (c) & (d) are for the IEEE 14-bus and 118-bus networks, respectively. (CC: Cyclic constraints, WCC: Without cyclic constraints.)

(i.e., when $\lambda = 1$ the load is increased by $100\%$ and when $\lambda = 2$, increased by $200\%$ and so on) for observing the impact of the bus voltage difference between two adjacent connecting buses and thus tightness of the proposed model. For the IEEE 14-bus network's overload condition, the voltage difference between bus no. 1 and bus no. 2 is low. Hence, the solution gap ($\sigma$) is low, and while the cyclic constraints are applied, the OPF model is tighter, which is shown in Fig. 10 (a)-(b). The metric $\sigma$ presents the overall tightness, with close to zero being tighter and thus more accurate. To illustrate the effect of a more extensive network, bus no. 43 and bus no. 44 in the IEEE 118-bus network are considered. The solution gap is checked by assessing the voltage difference for both conditions (i.e., with and without imposing the cyclic constraints). When there is a load increase (considered as the multiplying factor $\lambda \in [0, 3]$). The results show that the model is tight with CC and WCC when the voltage difference between two adjacent buses is small. However, with a larger voltage difference between adjacent buses, the solution gap is comparatively higher when cyclic constraints are not considered. This impact is observed on other buses as well. The solution gap from the proposed SOCP-OPF model is significantly lower, as shown in Fig. 10 (c)-(d). These results show that the proposed architecture is tight even for bi-directional flow if the cyclic constraints are applied with the OPF model.

## VI. Conclusion

This paper represents a novel branch flow-based SOCP-OPF model for meshed power transmission networks. A convex envelope is derived to satisfy cyclic angle constraints in meshed power networks. The tightness of the proposed OPF model and the solution gap is improved when the cyclic angle constraints are imposed. The condition for the proposed SOCP-OPF model's tightness for bi-directional power flow through a branch is also analyzed. The OPF model has been simulated

and evaluated for several IEEE standard meshed transmission test networks and compared with NLP-OPF and SDP-OPF models. From the simulation analysis, the proposed model is tight and provides a globally optimal solution. Furthermore, the computational efficiency and solution time for convergence of the proposed SOCP-OPF is improved by up to 58% when compared to the NLP-OPF and SDP-OPF models for large networks. In future work, the proposed OPF model will be extended for the mixed-integer version of OPF analysis and contingency analysis for unbalanced power networks.

## APPENDIX A

### A. Derivation of the Envelope for the $\theta_{ij}$:

The following convex envelope in (42)-(43) encloses the sine function in a polyhedral set as follows [33]:

$$\sin\theta_{ij} \leq \cos(\frac{\theta_{ij}^m}{2})(\theta_{ij} - \frac{\theta_{ij}^m}{2}) + \sin(\frac{\theta_{ij}^m}{2}) \tag{42}$$

$$\sin\theta_{ij} \geq \cos(\frac{\theta_{ij}^m}{2})(\theta_{ij} + \frac{\theta_{ij}^m}{2}) - \sin(\frac{\theta_{ij}^m}{2}) \tag{43}$$

where $\theta_{ij}^m = max[|\underline{\theta_{ij}}|, |\overline{\theta_{ij}}|]$.

Power transmission system networks are commonly in mesh orientation. For transmission networks, as the bus voltage (p.u) maximum and minimum limits are near unity and usually, the voltage (p.u) maximum and minimum limit of $[\underline{V}, \overline{V}] = [0.9, 1.1]$. If, $V_iV_j\sin\theta_{ij} = M$, then within the voltage limit, the $\sin\theta_{ij}$ function is relaxed as, $\sin\theta_{ij} \geq \frac{M}{\overline{V}_i\overline{V}_j}$ and $\sin\theta_{ij} \leq \frac{M}{\underline{V}_i\underline{V}_j}$. Then from (42):

$$\begin{aligned}
&\frac{M}{\overline{V}_i\overline{V}_j} \leq \cos(\frac{\theta_{ij}^m}{2})(\theta_{ij} - \frac{\theta_{ij}^m}{2}) + \sin(\frac{\theta_{ij}^m}{2}) \\
&\Rightarrow \theta_{ij} - \frac{\theta_{ij}^m}{2} \geq \frac{M}{\overline{V}_i\overline{V}_j\cos\frac{\theta_{ij}^m}{2}} - \tan\frac{\theta_{ij}^m}{2} \\
&\Rightarrow \theta_{ij} \geq \frac{M}{\overline{V}_i\overline{V}_j\cos\frac{\theta_{ij}^m}{2}} - \tan\frac{\theta_{ij}^m}{2} + \frac{\theta_{ij}^m}{2}
\end{aligned} \tag{44}$$

From (43):

$$\begin{aligned}
&\frac{M}{\underline{V}_i\underline{V}_j} \geq \cos(\frac{\theta_{ij}^m}{2})(\theta_{ij} + \frac{\theta_{ij}^m}{2}) - \sin(\frac{\theta_{ij}^m}{2}) \\
&\Rightarrow \theta_{ij} + \frac{\theta_{ij}^m}{2} \leq \frac{M}{\underline{V}_i\underline{V}_j\cos\frac{\theta_{ij}^m}{2}} + \tan\frac{\theta_{ij}^m}{2} \\
&\Rightarrow \theta_{ij} \leq \frac{M}{\underline{V}_i\underline{V}_j\cos\frac{\theta_{ij}^m}{2}} + \tan\frac{\theta_{ij}^m}{2} - \frac{\theta_{ij}^m}{2}
\end{aligned} \tag{45}$$

where $M = V_iV_j\sin(\theta_{ij}) = \frac{(B_{ij}P_{ij} - G_{ij}Q_{ij})}{(G_{ij}^2 + B_{ij}^2)}$.

### B. Convexity of the Proposed Envelope

The envelope in (44) and (45) are represented as follows:

$$\begin{aligned}
f_1(P,Q) &= \alpha(B_{ij}P_{ij} - G_{ij}Q_{ij}) + \beta_1 \\
f_2(P,Q) &= \alpha(B_{ij}P_{ij} - G_{ij}Q_{ij}) + \beta_2
\end{aligned}$$

where $\alpha = \frac{1}{\underline{V}_i\underline{V}_j\cos\frac{\theta_{ij}^m}{2}}$; $\beta_1 = -\tan\frac{\theta_{ij}^m}{2} + \frac{\theta_{ij}^m}{2}$ and $\beta_2 = \tan\frac{\theta_{ij}^m}{2} - \frac{\theta_{ij}^m}{2}$. $f(P,Q)$ can be split into two first-order functions as, $f(P,Q) = f(P) + f(Q)$. From the definition, a first-order equation can be considered as convex. In this article the envelope formed by $f(P,Q)$ is used for the relaxation of $\theta_{ij}$ from (6) as, $f_1(P,Q) \leq \theta_{ij} \leq f_2(P,Q)$.

## REFERENCES


[1] J. Momoh, R. Adapa, and M. El-Hawary, "A review of selected optimal power flow literature to 1993. i. nonlinear and quadratic programming approaches," *IEEE Transactions on Power Systems*, vol. 14, no. 1, pp. 96–104, 1999.

[2] K. Pandya and S. Joshi, "A survey of optimal power flow methods," *Journal of Theoretical and Applied Information Technology*, vol. 4, p. 450–458, 01 2008.

[3] S. Frank, I. Steponavice, and S. Rebennack, "Optimal power flow: a bibliographic survey i," *Energy systems*, vol. 3, no. 3, pp. 221–258, 2012.

[4] K. Lehmann, A. Grastien, and P. Van Hentenryck, "Ac-feasibility on tree networks is np-hard," *IEEE Transactions on Power Systems*, vol. 31, 10 2014.

[5] D. Bienstock and A. Verma, "Strong np-hardness of ac power flows feasibility," *Operations Research Letters*, vol. 47, no. 6, pp. 494–501, 2019. [Online]. Available: https://www.sciencedirect.com/science/article/pii/S0167637719302470

[6] P. Panciatici, M. C. Campi, S. Garatti, S. H. Low, D. K. Molzahn, A. X. Sun, and L. Wehenkel, "Advanced optimization methods for power systems," in *2014 Power Systems Computation Conference*, 2014, pp. 1–18.

[7] A. Castillo and R. P. O'Neill, "Survey of approaches to solving the ac opf," *US Federal Energy Regulatory Commission, Tech. Rep*, 2013.

[8] B. Stott, J. Jardim, and O. Alsac, "Dc power flow revisited," *IEEE Transactions on Power Systems*, vol. 24, no. 3, pp. 1290–1300, 2009.

[9] J. A. Taylor, *Convex optimization of power systems*. Cambridge University Press, 2015.

[10] Y. Weng, Q. Li, R. Negi, and M. Ilić, "Semidefinite programming for power system state estimation," in *2012 IEEE Power and Energy Society General Meeting*, 2012, pp. 1–8.

[11] B. Zhang, A. Lam, A. Dominguez-Garcia, and D. Tse, "Optimal distributed voltage regulation in power distribution networks," 04 2012.

[12] S. Moghadasi,and S. Kamalasadan, "Optimal fast control and scheduling of power distribution system using integrated receding horizon control and convex conic programming," *IEEE Transactions on Industry Applications*, vol. 52, no. 3, pp. 2596–2606, 2016.

[13] C. Coffrin, H. L. Hijazi, and P. Van Hentenryck, "The qc relaxation: A theoretical and computational study on optimal power flow," *IEEE Transactions on Power Systems*, vol. 31, no. 4, pp. 3008–3018, 2016.

[14] M. R. Narimani, D. K. Molzahn, and M. L. Crow, "Tightening qc relaxations of ac optimal power flow problems via complex per unit normalization," *IEEE Transactions on Power Systems*, vol. 36, no. 1, pp. 281–291, 2021.

[15] D. Lee, K. Turitsyn, D. K. Molzahn, and L. A. Roald, "Robust ac optimal power flow with robust convex restriction," *IEEE Transactions on Power Systems*, vol. 36, no. 6, pp. 4953–4966, 2021.

[16] S. H. Low, "Convex relaxation of optimal power flow—part i: Formulations and equivalence," *IEEE Transactions on Control of Network Systems*, vol. 1, no. 1, pp. 15–27, 2014.

[17] S. H. Low, "Convex relaxation of optimal power flow—part ii: Exactness," *IEEE Transactions on Control of Network Systems*, vol. 1, no. 2, pp. 177–189, 2014.

[18] R. Jabr, "Radial distribution load flow using conic programming," *Power Systems, IEEE Transactions on*, vol. 21, pp. 1458 – 1459, 09 2006.

[19] X. Bai, H. Weihua, K. Fujisawa, and Y. Wang, "Semidefinite programming for optimal power flow problems," *International Journal of Electrical Power Energy Systems*, vol. 30, pp. 383–392, 07 2008.

[20] R. A. Jabr, "A conic quadratic format for the load flow equations of meshed networks," *IEEE Transactions on Power Systems*, vol. 22, no. 4, pp. 2285–2286, 2007.

[21] B. Kocuk, S. Dey, and X. Sun, "Strong socp relaxations for the optimal power flow problem," *Operations Research*, vol. 64, 05 2016.

[22] M. Farivar and S. H. Low, "Branch flow model: Relaxations and convexification—part i," *IEEE Transactions on Power Systems*, vol. 28, no. 3, pp. 2554–2564, 2013.

[23] Farivar, Masoud and Low, Steven H., "Branch flow model: Relaxations and convexification—part ii," *IEEE Transactions on Power Systems*, vol. 28, no. 3, pp. 2565–2572, 2013.

[24] Z. Tian and W. Wu, "Recover feasible solutions for SOCP relaxation of optimal power flow problems in mesh networks," *IET Generation, Transmission Distribution*, vol. 13, no. 7, pp. 1078–1087, 2019.

[25] Z. Miao, L. Fan, H. G. Aghamolki, and B. Zeng, "Least squares estimation based sdp cuts for socp relaxation of ac opf," *IEEE Transactions on Automatic Control*, vol. 63, no. 1, pp. 241–248, 2018.

[26] A. F. Soofi, S. D. Manshadi, G. Liu, and R. Dai, "A socp relaxation for cycle constraints in the optimal power flow problem," *IEEE Transactions on Smart Grid*, vol. 12, no. 2, pp. 1663–1673, 2021.

[27] D. K. Molzahn, B. C. Lesieutre, and C. L. DeMarco, "A sufficient condition for global optimality of solutions to the optimal power flow problem," *IEEE Transactions on Power Systems*, vol. 29, no. 2, pp. 978–979, 2014.

[28] R. Madani, S. Sojoudi, and J. Lavaei, "Convex relaxation for optimal power flow problem: Mesh networks," *IEEE Transactions on Power Systems*, vol. 30, no. 1, pp. 199–211, 2015.

[29] D. K. Molzahn, J. T. Holzer, B. C. Lesieutre, and C. L. DeMarco, "Implementation of a large-scale optimal power flow solver based on semidefinite programming," *IEEE Transactions on Power Systems*, vol. 28, no. 4, pp. 3987–3998, 2013.

[30] B. C. Lesieutre, D. K. Molzahn, A. R. Borden, and C. L. DeMarco, "Examining the limits of the application of semidefinite programming to power flow problems," in *Proc. 49th Annual Allerton Conference on Communication, Control, and Computing (Allerton)*, 2011, pp. 1492–1499.

[31] M. M. U. T. Chowdhury and S. Kamalasadan, "An angle included optimal power flow (opf) model for power distribution network using second order cone programming (socp)," in *Proc. IEEE Industry Applications Society Annual Meeting*, 2020, pp. 1–7.

[32] T. Chowdhury and S. Kamalasadan, "A new second-order cone programming model for voltage control of power distribution system with inverter based distributed generation," *IEEE Transactions on Industry Applications*, pp. 1–1, 2021.

[33] D. K. Molzahn, I. A. Hiskens *et al.*, "A survey of relaxations and approximations of the power flow equations," *Foundations and Trends® in Electric Energy Systems*, vol. 4, no. 1-2, pp. 1–221, 2019.

[34] R. D. Zimmerman, C. E. Murillo-Sánchez, and R. J. Thomas, "Matpower: Steady-state operations, planning, and analysis tools for power systems research and education," *IEEE Transactions on Power Systems*, vol. 26, no. 1, pp. 12–19, 2011.

[35] S. Huang, Q. Wu, J. Wang, and H. Zhao, "A sufficient condition on convex relaxation of ac optimal power flow in distribution networks," *IEEE Transactions on Power Systems*, vol. 32, no. 2, pp. 1359–1368, 2017.

[36] A. B. Birchfield, T. Xu, K. M. Gegner, K. S. Shetye, and T. J. Overbye, "Grid structural characteristics as validation criteria for synthetic networks," *IEEE Transactions on Power Systems*, vol. 32, no. 4, pp. 3258–3265, 2017.